16th World Conference on Earthquake, 16WCEE 2017
Santiago Chile, January 9th to 13th 2017
Paper N° 645 (Abstract ID)
Registration Code: S-V1463022091

SEISMIC ASSESSMENT OF PERUVIAN CONFINED MASONRY DWELLINGS USING FRAGILITY FUNCTIONS

L. G. Quiroz[1], Y. Maruyama[2]

[1] Associated Researcher, Department of Earthquake Engineering, Japan-Peru Earthquake Engineering and Disaster Mitigation Center, Faculty of Civil Engineering, National University of Engineering, Lima-Peru, lgquiroz@uni.edu.pe.
[2] Associate Professor, Department of Urban Environment Systems, Chiba University, Japan, ymaruyam@faculty.chiba-u.jp.

Abstract

The evaluation of the seismic performance of buildings in seismic-prone regions is very important because the structures with inadequate seismic performance are the main causes of economic and human losses. Structural seismic performance can be evaluated using fragility functions, which allow the estimation of the probable damage due to a seismic event. In Lima, Peru, many dwellings are constructed with confined masonry (CM) walls. The low cost of this typology makes it the most representative and most extended construction system in the city for low-rise dwellings. In this study, an analytical approach was adopted to construct fragility functions for low-rise dwellings whose vertical and lateral resistance systems are CM walls. This structural system has been typically used since 1940. Numerical models based on the samples of one-, two-, and three-story dwellings were analyzed, and the properties of their main structural elements were defined based on the experimental results. A series of nonlinear dynamic analyses was performed using strong-motion records of seismic events around the world. Simulated ground motion records in Lima assuming the occurrence of an earthquake scenario were also employed. The fragility functions for the dwellings were constructed assuming that the damage ratios follow a lognormal distribution. The results show that one-story CM dwellings will perform in accordance with the Peruvian seismic design standard whereas two- and three-story dwellings will suffer irreparable damage.

Keywords: Confined masonry dwellings, Nonlinear dynamic analyses, Fragility functions.

1. Introduction

The correlation of the severity of the earthquake ground motion with the structural damage is the most common method of characterizing damage distribution in a region. Those correlations are derived as damage probability distributions at specific ground motion intensities, and are usually presented as fragility functions for different structural systems. Fragility functions describe the conditional probability of a structure sustaining different damage states at given levels of ground motion intensity, which is expressed by Eq. (1):

$$P_{ik} = P\left[X \geq x_i \middle| Y = y_k\right] \quad (1)$$

where P_{ik} is the conditional probability of the degree of damage x_i at ground motion intensity level y_k; and X and Y are the variables representing the damage state and ground motion intensity, respectively.

In the urban areas of Latin America, structures are widely built using confined masonry (CM) walls and hence, estimating the loss related to their damage is very critical. This type of construction deploys masonry units with vertical RC tie-columns that confine the brick walls and RC bond-beams along the walls at floor level. Several low-rise CM dwellings have been built in Lima city since 1940 (Fig. 1) and their number has been increasing because of the low cost of construction. Because no strong earthquake has hit Lima since 1974, the actual behavior of such dwellings during seismic events and the potential losses associated with their failure are unknown.

The objective of this study is to evaluate the seismic performance of low-rise one-, two-, and three-story CM dwellings in Lima using analytical fragility functions, therefore a process of evaluating seismic loss using fragility functions is followed. It includes the following steps: definition and calibration of a numerical model, selection of intensity measure, calculation of structural responses, estimation of damage, statistical analysis of results, construction of fragility functions, and finally, loss assessment.

The seismic response of CM walls, which are regarded as archetypes of those used in low-rise dwellings in Lima, were evaluated in a previous study [1]. The numerical model of a wall in the dwellings was developed using a multi-degree-of-freedom (MDOF) system and macro models.

In light of the uncertainties surrounding earthquakes in a region, it is important to select a representative set of records that cover the maximum number of uncertainties. Therefore, the number of actual records selected for a given region of study must account for all conditions of regional seismicity and the effects of local geology. In Peru, the number of seismic motion records available is very limited compared to that in countries such as USA and Japan. Petrovski and Nocevski [2] selected three real seismic records whereas Hwang and Huo [3] used synthetic earthquakes records. It is also necessary to select a suitable damage indicator that can characterize the magnitude of damage during an earthquake. Local damage index (for various structural elements) and global damage index (for the entire structure) are amongst the many damage indices available. The different damage indices have been reviewed in a previous study [4].

Real ground motion records of seismic events in different countries and simulated records for Lima were examined for selecting the two abovementioned parameters. A suitable damage indicator was selected from the available literature and validated by comparing it with the results of previously conducted experiments on CM structures in Lima [5].

A series of nonlinear dynamic response analyses was performed using the ground motion records of overseas events. Simulated ground motion records assuming a scenario earthquake event in Peru [6] were also considered for performing dynamic response analyses. Regression analyses were performed to compare the building damage ratios with ground motion indices to, in turn, construct the fragility functions. Finally, using these functions, the seismic performance of low-rise dwellings was evaluated for three hazard levels, and the weighted mean damage was estimated. No studies on the generation of analytical fragility functions for CM dwellings in Lima are available.

Fig.1. Typical CM dwellings in Lima, Peru.

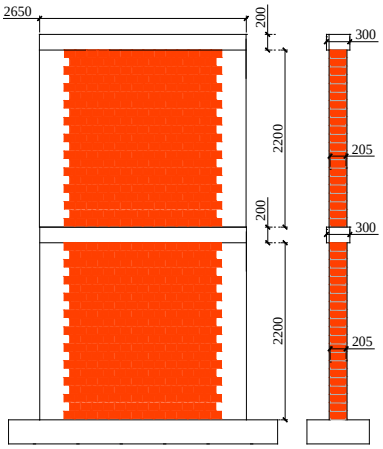

Fig. 2. Two-story numerical model (general geometry)

2. Numerical modeling

The shapes of the dwellings in Lima are mostly rectangular. Muñoz et al. [7] presents the architectural drawings of a typical two-story CM dwelling. The distribution of the structural elements may be considered the same in all stories in one-, two-, and three-story dwellings. The wall density is larger in the longitudinal direction of the dwellings and hence, the structure is significantly stronger and stiffer in that direction perpendicular to the street. In the weaker direction (parallel to the street), the structural axes are composed of one or two CM walls. The analysis was conducted considering a single wall in the weeker direction of the structure.

The geometry and dimension of the analyzed model of two-story dwellings is schematically shown in Fig. 2. The general dimensions of the CM walls and their confinement elements considered for analysis were set to be as close as possible to those of real low-rise dwellings. The number of stories considered was between 1 and 3. The walls were assumed to be monolithically connected to the foundation and founded in firm soil. A similar distribution was considered for the one- and three-story dwellings. The dimensions and reinforcements of the confining elements are listed in Table 1.

The analytical model considered the effects of nonlinearity in the masonry panel by using two diagonal compression struts per story (Fig. 3), which imparted lateral resistance to cyclic loading. Because of the negligible tensile strength of the masonry, the struts were considered to be ineffective in tension. The relationship between the struts' lateral load and displacement is given by a curve bounded by a strength envelope, which is defined by the initial elastic stiffness of the panel K_o until subjected to a yield force V_y. The force after yielding is defined by a degraded stiffness until the panel is subjected to the maximum force V_m (Fig. 3) [8].

Table 1. Dimensions and reinforcements of confining elements in numerical models.

Tie-column				Bond-beam			
T (mm)	B (mm)	Longitudinal Reinforcement	Transverse Reinforcement	h (mm)	b (mm)	Longitudinal Reinforcement	Transverse Reinforcement
230	300	4 #4 [a]	#2: 1@5 cm, 4@10 cm, rest@25 cm	200	300	4 #3 [b]	#2: 1@5 cm, 4@10 cm, rest@25 cm

[a] 4 #4: Four conventional rebars 12.7 mm in diameter in the section of the element.
[b] 4 #3: Four conventional rebars 9.5 mm in diameter in the section of the element.

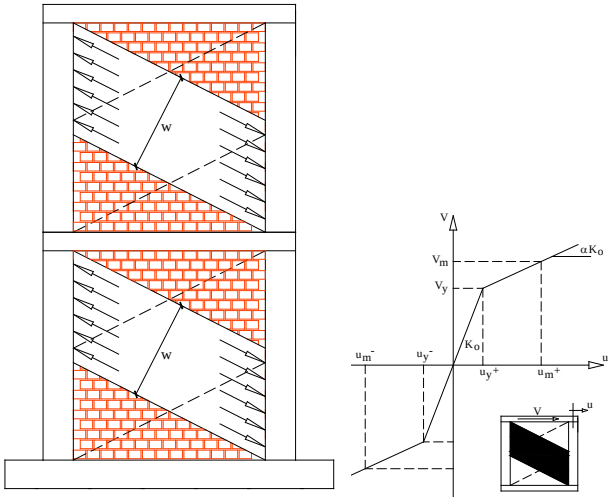

Fig. 3. (a) Equivalent strut model for masonry panels and strength envelope for struts [8].

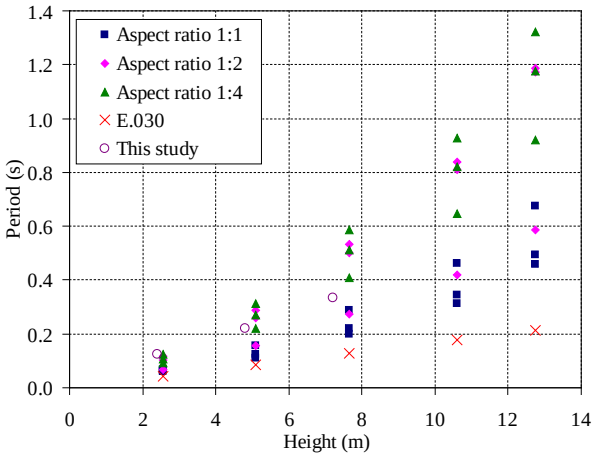

Fig. 4. Comparison of natural periods given by Proaño and Zavala [11], and current study, with respect to height of dwellings.

The value of K_o can be calculated using Eq. (2):

$$K_o = E_m \times A / L \tag{2}$$

where E_m is the modulus of elasticity of the masonry, and A and L are the area and length of the equivalent strut, respectively. The value of A can be estimated using Eq. (3)

$$A = w \times t \tag{3}$$

where w is the width of the strut and t is the thickness of the wall. In the present study, the definition provided by Bazan and Meli [9] for the width of the strut was employed. Value of *Vy* was estimated as defined in Peruvian standard E.070 [10]. Similar procedures were followed to estimate the properties of the struts for the one-, two- and three-story numerical models.

The tie-column elements were considered as macro-elements with inelastic flexural deformations, and elastic shear and axial deformations. The bond-beam elements were modeled using a nonlinear flexural stiffness model and linear elastic shear deformations. The hysteretic response of an RC section was traced using a three-parameter model that considered a trilinear polygonal skeleton along with stiffness degradation, strength deterioration, and pinching response. The concrete was assumed to be confined, and the Kent and Park model was employed to study its behavior.

The hysteretic model used for masonry panels includes the effects of stiffness degradation, strength deterioration, and pinching, and is based on 12 parameters [8]. The values of these parameters were estimated using the test results and genetic algorithms of a calibration process [1].

For estimating the loads in the structure, the gravity loads per unit area were regarded as distributed dead loads with magnitudes 2870, 1000, and 1000 N/m^2 resulting from the weight of the concrete slab, non-structural partitions, and floor finishings, respectively. The live load per unit area was considered as 2500 N/m^2 for all stories except the top level, for which 1000 N/m^2 was considered.

The natural periods of the one-, two-, and three-story numerical models were obtained as 0.16, 0.24, and 0.37 s, respectively. Figure 4 shows a comparison of the periods obtained in this study with those obtained by Proaño and Zavala [11] with respect to the height of dwellings. It also shows that the values obtained for the numerical models in this study are similar to those obtained in other studies.

Table 2. Definitions of damage states for various interstory drifts.

State	Interstory Drift (%)	Description	Damage state
1	0–0.125	No damage	No damage (ND)
2	0.125–0.286	Commencement of diagonal cracking	Light (L)
3	0.286–0.5	Initial cracking of tie-columns and opening of diagonal cracks	Severe (S)
4	>0.5	Horizontal cracks along tie-columns and generalization of diagonal cracks	Collapse (C)

3. Damage states and input ground motions

3.1 Damage states and damage indices

The experimental results indicated that damage to structures is directly related to local deformations [5]. Hence, interstory drift can be used to indicate a specific damage state and is calculated as the ratio of a story's relative displacement to its height.

In 2004, Zavala et al. [5] found that a two-story masonry dwelling using handmade bricks behaves elastically until an interstory drift of 0.0625% and that its walls begin cracking after an interstory drift of 0.125%, through a full-scale test conducted in the structure laboratory of the Peru-Japan Center for Seismic Research and Disaster Mitigation, CISMID. They also found that the specimen underwent high deterioration under an interstory drift of 0.50%. In the present study, the drift thresholds corresponding to the significant damage states were considered based on the experiments by Zavala et al. [5]. Table 2 lists the definitions of damage states for various interstory drifts.

3.2 Input ground motion records and seismic intensity

The uncertainty related to ground motion can be overcome by considering various records reflecting the real seismicity of a region. Initially, the select real seismic records in Lima was attempted to overcome this uncertainty but the number of records per seismic event in Peru was found to be very limited compared to that of other countries. Moreover, the available records of past events presented low PGAs (<100 cm/s^2). Therefore, the ground motion records of seismic events in Japan, USA, Taiwan, and Chile were used in this study. The following earthquakes were considered: Chibaken-Toho-Oki (1987), Kobe (1995), Northridge (1994), Chi-Chi (1999), Tohoku (2011), and Maule (2010). The records of the first four earthquakes were compiled mainly by Karim and Yamazaki [12, 13]. Records of recent major seismic events with large PGAs were also considered: 19 and 25 records of the Maule (2010) and Tohoku (2011) earthquakes, respectively. Lastly, the 10 records of Lima city events simulated by Pulido et al. [6] were also considered for the study. Only horizontal components were used as input motions.

Many characteristics of the records were studied including PGA, PGV, root-mean-square acceleration (A_{RMS}), root-mean-square velocity (V_{RMS}), arias intensity (AI), acceleration spectrum intensity (ASI), velocity spectrum intensity (VSI), and period. Table 3 lists only PGA, PGV, ARMS and VRMS for the last three groups of ground motion records in terms of a range of seismic indices.

It is important to select an appropriate intensity indicator that has good correlation with structural damage. Typically, PGA is used as the seismic intensity index but a high PGA is not always associated with severe structural damage [12]. The other parameters that can be used to represent seismic intensity include PGV, AI, Sa (T1, 5%), duration, and values in the modified Mercalli intensity scale.

For selecting an appropriate intensity measure, a nonlinear analysis of the relationship between the maximum interstory drift in a two-story model and the characteristics of the records was performed using the univariate regression model shown in Eq. (4).

Table 3. Range of seismic indices of ground motion records used in this study.

Parameter (Unit)	PGA (cm/s^2)	PGV (cm/s)	A_{RMS} (cm/s^2)	V_{RMS} (cm/s)
Tohoku	[427.87–2733.78]	[16.60–107.16]	[30.92–164.62]	[1.92–7.18]
Maule	[73.35–913.26]	[5.78–58.70]	[11.60–92.68]	[1.26–13.01]
Peru-simulated	[288.14–847.70]	[14.55–101.92]	[32.64–82.10]	[2.36–9.41]

$$y = ax^b \tag{4}$$

where y and x represent the indices of damage (maximum interstory drift) and strong motion (e.g., PGA, PGV, and VSI) respectively, and a and b are the regression coefficients. Figure 5 shows the relationships between the maximum interstory drift and values of PGA for the two-story numerical model, as well as their respective coefficients of determination (R^2). The damage index is seen to have the highest correlation with PGA ($R^2 = 0.86$), and therefore, the latter was selected as the intensity measure.

Figure 6 presents the acceleration response spectra for simulated records of Lima. The curves were normalized to have a PGA of 1 g for the purpose of comparing them with the results obtained by Karim and Yamazaki [12]. The blue and red lines in the figure represent the mean amplitude of each event and the design acceleration response spectrum according to the E.030 [14], respectively. The expression proposed by Iervolino et al. [15] was employed for evaluating the extent of deviation of record's mean spectrum from its code spectrum. This expression calculates the average spectrum deviation δ as in Eq. (5).

$$\delta = \sqrt{\frac{1}{N}\sum_{i=1}^{N}\left(\frac{Sa_j(T_i) - Sa_{reference}(T_i)}{Sa_{reference}(T_i)}\right)^2} \tag{5}$$

where $Sa_j(T_i)$ is the pseudo-acceleration ordinate of the real spectrum j, corresponding to the period T_i, $Sa_{reference}(T_i)$ is the value of the spectral ordinate of the target spectrum for the same period, and N is the number of spectral ordinates within the considered range of periods. For the present study, we limited the range of periods to $0.2T_1$ and $1.5T_1$, where T_1 is the natural period of the numerical model in the first mode. Equation 5 gave lowest value for the simulated records of Lima in case of one- and two-story models, but for the three-story model, the value of δ was the smallest for the Maule earthquake records.

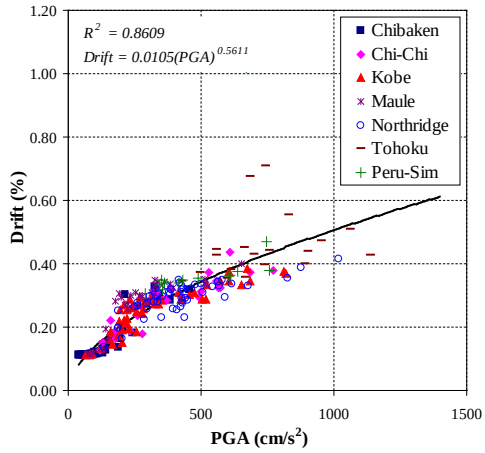

Fig. 5. Relationships between damage index and values of PGA for the two-story numerical model.

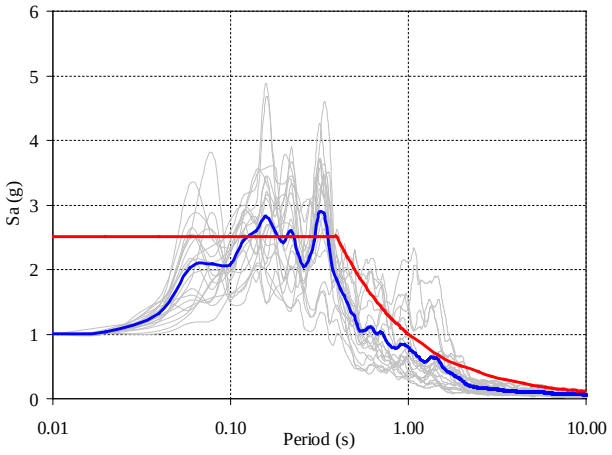

Fig. 6. Normalized acceleration response spectra corresponding to 5% damping ratio for earthquakes considered in Peru-simulated records.

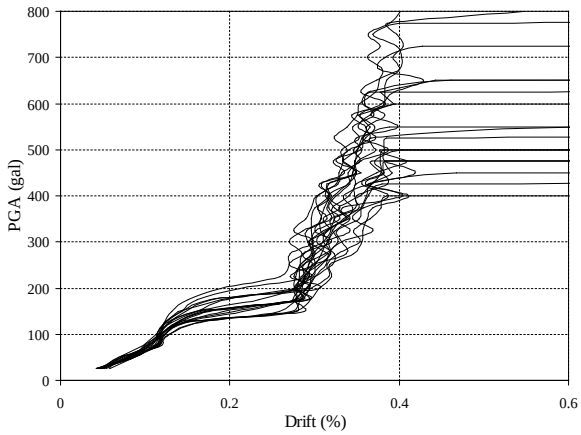

Fig. 7. Comparison of maximum interstory drift for two-story numerical model using simulated records for Lima

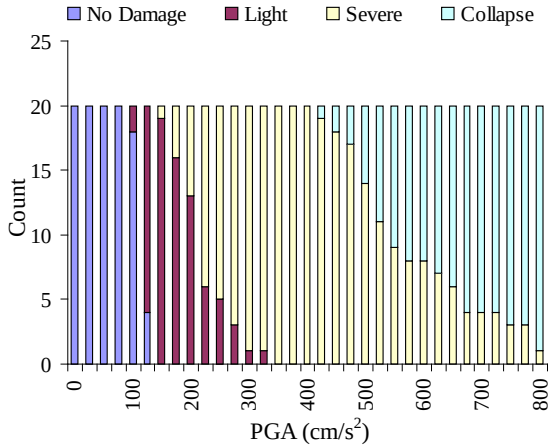

Fig. 8. Frequencies of occurrence of each damage state based on Peruvian simulated records, for two-story numerical model

These results indicate that the mean amplitude of the normalized acceleration response spectra in the simulated records for Lima matched better with the Peruvian design spectra for one- and two-story dwellings whereas for three-story dwellings, the records of the Maule earthquake match better.

4. Dynamic response analysis and construction of fragility functions

Nonlinear dynamic response analyses of the numerical models were conducted using a combination of Newmark-beta integration and the pseudoforce method in the IDARC program. Every record was scaled to different excitation levels for obtaining the frequencies of occurrence of each damage state. In the present study, the PGA of every record was scaled from 25 cm/s^2 until three times its original PGA [16] at an interval of 25 cm/s^2. The scaled records were applied to the numerical models to obtain the maximum interstory drift. Figure 7 shows the plot of the maximum interstory drift observed in the two-story numerical model, for different simulated input-scale ground motion records for Lima. The maximum interstory drift of the numerical model are observed to be different for every simulated record even at the same intensity level (PGA). This finding confirms that the periodic characteristics of input ground motion records affect the structural response. Similar observations were made for the other events and numerical models.

Then, the frequency of occurrence of each damage state was obtained for each excitation level. Finally, the damage ratio was calculated for every damage state. Figure 8 presents the frequency of occurrence of every damage state with respect to the PGA for the numerical model for the Peruvian simulated records for the two-story numerical model, as an example. It is observed that the frequency of no-damage occurrence decreases whereas that of collapse occurrence increases with increase in the excitation level.

For constructing the fragility functions, lognormal probability distribution between the PGA and damage ratio was assumed [17]. The cumulative probability P_R of an event meeting or exceeding the condition for a particular damage state is defined by Eq. (6):

$$P_R = \Phi\left[\frac{\ln Y - \lambda}{\zeta}\right] \tag{6}$$

where Φ is the standard cumulative normal distribution function, Y is the ground motion index (PGA), and λ and ζ are the two statistical parameters of the distribution (i.e., the mean and standard deviation of ln Y, respectively) obtained by plotting ln Y against the inverse of Φ on a lognormal probability paper. The values of λ and ζ are obtained using the least-squares method.

Table 4. Parameters of fragility functions for two-story numerical model across each event.

Event	Damage state (DS)					
	DS > Light		DS > Severe		DS = Collapse	
	λ	ζ	λ	ζ	λ	ζ
Maule	4.72	0.11	5.49	0.21	6.39	0.24
Tohoku	4.74	0.19	5.40	0.30	6.22	0.30
Peru-simulated	4.72	0.09	5.36	0.23	6.36	0.22

Using the previously discussed procedure, the statistical parameters defining the fragility functions were estimated for every event and numerical model. Table 4 lists the values of λ and ζ for Maule, Tohoku and Peruvian simulated records for the two-story numerical model.

5. Analysis of fragility functions

5.1 Influence of input ground motion records

Figure 9 presents the fragility functions for severe and collapse damage states and every event for the two-story numerical model, respectively. In the three-story numerical model, there was no occurrence of light damage for any event. In one-story numerical model, only the light damage state occurred. It was observed that the probability of an event meeting or exceeding the condition for a damage state varies across events, particularly for the collapse damage state.

The simulated ground motion records presented the highest probability of event occurrence in the severe damage state whereas the Northridge event presented the lowest. The probability of the Tohoku event meeting or exceeding the condition for collapse damage state was higher than that of any other event. In the three-story numerical model, the probability of meeting or exceeding the severe and collapse damage state conditions is seen to be high for the Tohoku earthquake and simulated ground motion records for Lima. In the case of three-story numerical model, the fragility functions of all events except the Kobe and Northridge earthquakes rapidly change from the severe to collapse damage states, indicated by the closeness of the two damage states and steepness of their slopes.

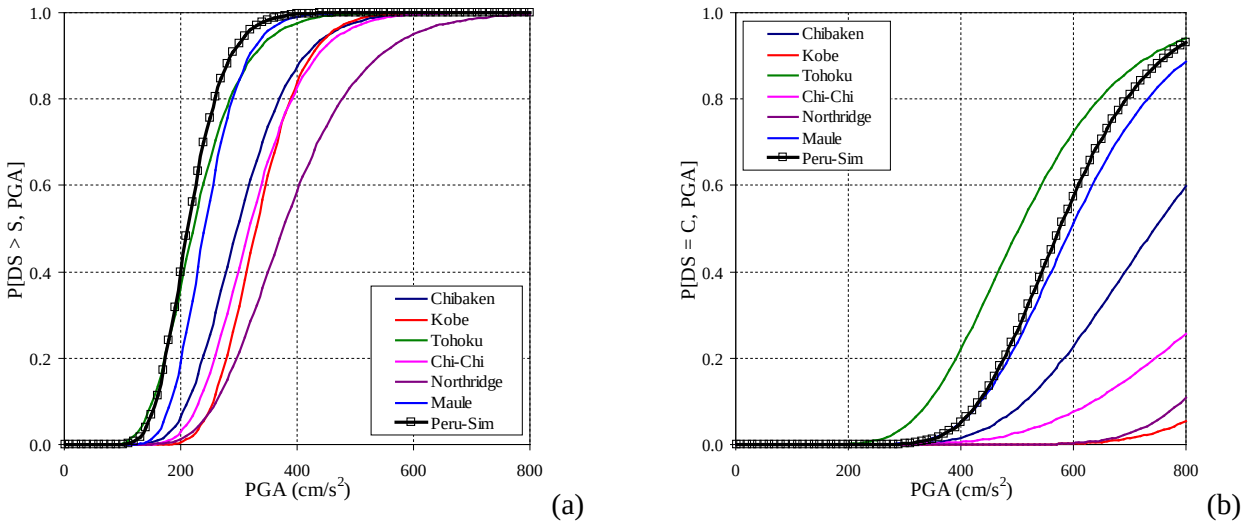

Fig. 9. Comparison of fragility functions of various earthquake events across damage states for two-story numerical model: a) severe, and b) collapse

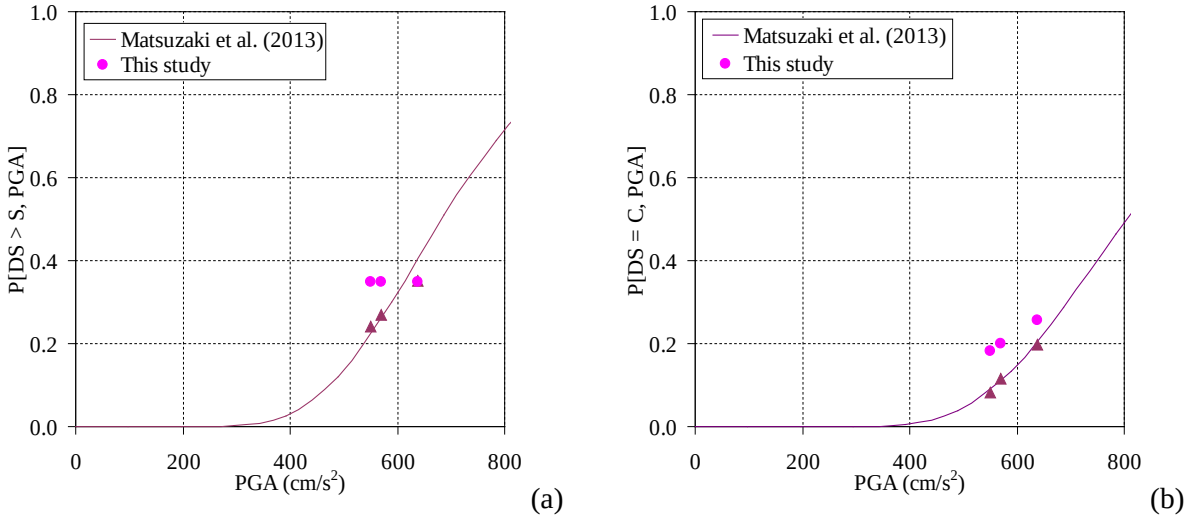

Fig. 10. Comparison of fragility functions developed by Matsuzaki et al. [19] with those obtained in this study.

This effect could imply that the structure is susceptible to soft-story collapse [18]. From figure 9, it can be observed that fragility functions depend on the spectral characteristics of earthquake ground motion and other properties such as period and excitation level. This dependence confirms that the input motion records used in the construction of fragility functions must adequately represent the seismicity in the region of study.

5.2 Validation of fragility functions

Matsuzaki et al. [19] constructed fragility functions in terms of PGA and PGV for brick-masonry buildings in Pisco city, based on damage survey data and seismic ground motion records simulated. The mix of dwellings considered in that study were 65% one-story, 29% two-story, and 6% three-or-more-stories dwellings. The authors obtained three damage ratios for constructing the fragility functions under associated excitation levels for PGA values of 0.56, 0.58 and 0.65 g. Applying the fragility curves estimated in Section 4 and using the abovementioned mix of dwellings, the probabilities of the event meeting or exceeding the condition for severe and collapse damage states were estimated and compared with those presented by Matsuzaki et al. [19]. Figure 10 shows a comparison of both results. The estimations using the fragility curves in this study are a little higher. This can be explained by the fact that adjacent dwellings in Pisco are constructed without gaps between each other and hence, their total possible displacement and the associated damage could be smaller than those estimated in the present study.

6. Evaluation of seismic performance

In the present study, the seismic hazard (seismicity) levels suggested by the Structural Engineers Association of California [20] were used. These levels are defined as occasional, rare, and very rare earthquakes having 50%, 10%, and 5% exceedance in 50 years, respectively. Table 5 lists the PGA values for the defined three levels of seismicity.

Table 5. PGA associated with different levels of seismicity.

Seismic Hazard Level		PGA (g)	Return period (years)
Occasional Eq.	(50% of exceedance / 50 years)	0.20	72
Rare Eq.	(10% of exceedance / 50 years)	0.40	475
Very rare Eq.	(5% of exceedance / 50 years)	0.50	975

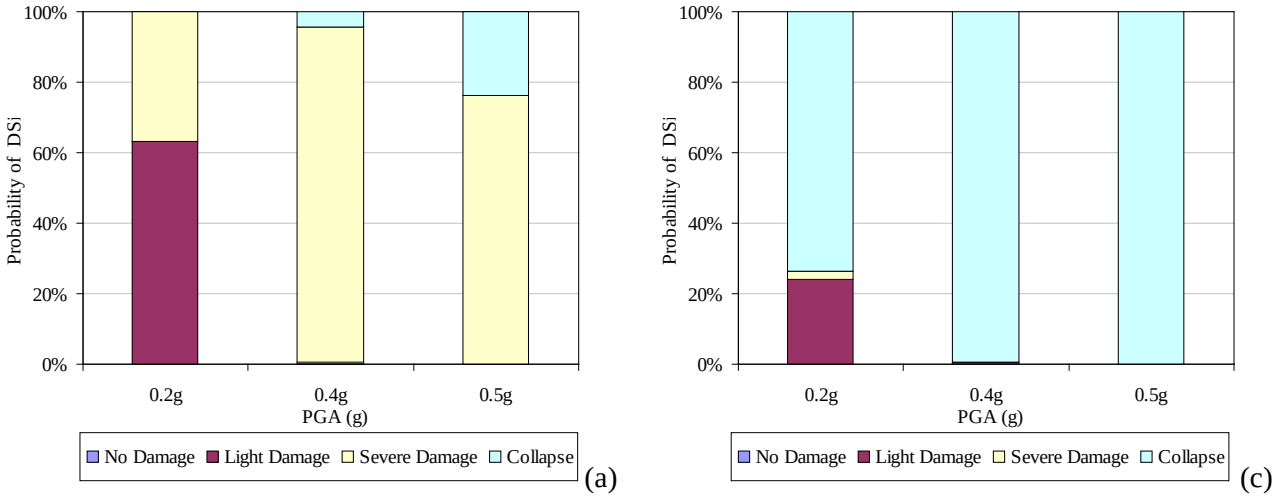

Fig. 11. Damage probabilities for a) two-story, and b) three-story dwellings corresponding to PGAs of 0.2 g, 0.4 g, and 0.5 g.

The E.030 [14] requires that structures support moderate earthquake (0.2 g) with the possibility of minor structural damage and severe earthquakes (0.4 g) without collapse. E.030 does not present provisions for very rare earthquakes. Using the fragility functions obtained for the simulated ground motion records for Lima, the probability of occurrence of each damage state at each specific hazard level was calculated.

Figure 11 shows a comparison of the damage probabilities with respect to the PGA for the three ground motion intensity levels for two- and three-story numerical models developed using the simulated records for Lima. The findings indicate that only one-story dwellings in Lima will meet the E.030 requirement. The probability of collapse of two-story dwellings due to rare earthquake events is low and the probability of severe damage due to occasional earthquakes is relatively higher. In case of three-story dwellings, the probability of collapse is high even for the occasional earthquake.

The weighted mean damage state D_m [21] was also used for evaluating the seismic performance of the dwellings, which is calculated using Eq. (7):

$$D_m = \left(\frac{1}{3}\right)\sum_{i=0}^{3} DS_i P[DS_i] \tag{7}$$

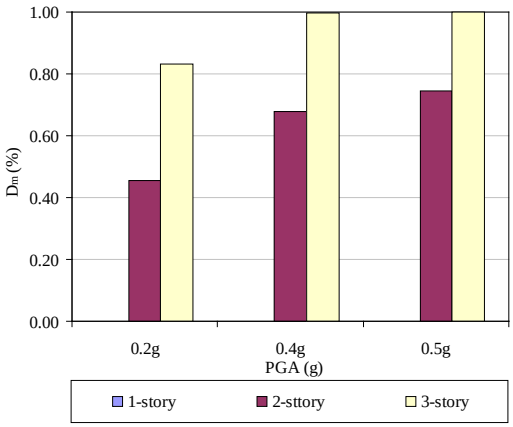

Fig. 12. Weighted mean damage for three levels of ground motion intensity (0.2 g, 0.4 g, and 0.5 g) for all numerical models.

where DS_i takes the values 0, 1, 2, and 3 in accordance with the damage states represented by *i*, and $P[DS_i]$ represents the corresponding probability. The value of D_m is the closest to the most likely damage state of a structure. Figure 12 shows the discrete values of D_m for the three levels of intensity across all models developed using the simulated records for Lima.

According to the ATC-21 project [22], damage to a structure may be irreparable if the mean damage is greater than 60%. According to Fig. 12, the one-story dwellings would suffer no damage whereas two-story dwellings would suffer irreparable damage due to rare and very rare earthquakes. In three-story dwellings, the damage would be irreparable for the three levels of intensity. These estimations for two- and three-story dwellings using the fragility curves or weighted mean damage methods may be regarded high but as stated in Section 5.2, the dwellings are constructed in a block without considering seismic joints, due to which their lateral displacements and thereby, the expected damage are reduced.

8. Conclusions

As fragility functions are effective tools (considering that the uncertainty related to ground motion prediction can be handled using probabilistic procedures), they were used for estimating structural damage in low-rise CM dwellings in Lima.

From the obtained variations in input ground motion records, it was observed that the values of the statistical parameters defining the fragility functions depend on the characteristics of the record and the excitation level. This observation confirms the idea of using a group of records that reflect the specific seismicity of the region under study.

The study revealed that one-story dwellings will suffer no damage whereas two-story dwellings will have over 60% and less than 36% probabilities of suffering light and severe damage, respectively, due to occasional earthquakes. This indicates that two-story dwellings in Lima will not accomplish the requirements of the E.030. The probability of collapse of these dwellings due to rare earthquakes was estimated to be less than 5%. Although the E.030 stipulates zero probability of collapse for this case, the value obtained from the analysis may be considered adequately low. The findings also indicate that three-story dwellings will suffer strong damage even under occasional earthquakes and hence, will not accomplish the E.030 requirements.

The analysis of the weighted mean damage revealed that two- and three-story dwellings would suffer irreparable damage, as per the ATC-21 project. These values may be considered to be high (especially for three-story dwellings) but also conservative because these dwellings are regarded to be constructed separately from seismic joints, allowing complete lateral displacement. In reality, however, dwellings are built next to each other, owing to which the lateral displacement and damage are reduced.

9. References

[1] Quiroz L, Maruyama Y and Zavala C (2014): Cyclic behavior of Peruvian confined masonry walls and calibration of numerical model using genetic algorithms. *Engineering Structures* **75**, 561–576.

[2] Petrovski S and Nocevski NK (1993): Definition of empirical and theoretical models for assessment of vulnerability level in high rise buildings. *Technical Report*, IZIIS, Skopje.

[3] Hwang HHM and Huo JR (1994): Generation of hazard-consistent fragility curves. *Soil Dynamics and Earthquake Engineering* **13**, 345–354.

[4] Ghobarah A, Abou-Elfath H and Biddah A (1999): Response based damage assessment of structures. *Earthquake Engineering and Structural Dynamics* **28**, 79–104.

[5] Zavala C, Honma C, Gibu H, Gallardo J and Huaco G (2004): Full scale on line test on two story masonry building using handmade bricks. Proceedings of *15th World Conference on Earthquake Engineering*, Lisbon, Portugal. Paper No. 2885.

[6] Pulido N (2013): Earthquake rupture and slip scenarios for Central Andes Peru, and strong motion simulations for Lima (v1.0 February 7/2013). http://www.j-shis.bosai.go.jp/staff/nelson/smsimu_Central_Peru_v1p0/Lima_SMsimu_v1p0.htm.

[7] Muñoz A, Blondet M, Tarque N, Carpio J and Florez A (2009): Capacity spectra of a typical confined masonry dwelling in Peru. http://www.world-housing.net/wp-content/uploads/pager/2009/08/Capacity-curves-masonry-Peru.pdf

[8] Reinhorn AM, Roh H, Sivaselvan M, Kunnath SK, Valles RE, Madan A, Li C, Lobo R and Park YJ (2009): IDARC2D version 7.0: A program for the inelastic damage analysis of structures. *Technical Report, MCEER-09-0006*, State University of New York at Buffalo.

[9] Bazan M and Meli R (2009): *Seismic design of buildings*. Limusa Noriega Ed. Mexico. (In Spanish).

[10] SENCICO (2006): *Standard E.070 Masonry*. National Building Regulations, Lima, Peru. (In Spanish).

[11] Proaño R and Zavala C (2003): Estimation of the seismic response of structures based on SDOF systems for calculation of seismic vulnerability. Proceedings of the *14th National Conference of Civil Engineering*, Iquitos, Peru, Paper No. EM-38. (In Spanish)

[12] Karim K R and Yamazaki F (2001): Effect of earthquake ground motions on fragility curves of highway bridge piers based on numerical simulation. *Earthquake Engineering and Structural Dynamics* **30** (12), 1839–1856.

[13] Karim K R and Yamazaki F (2003): A simplified method of constructing fragility curves for highway bridges. *Earthquake Engineering and Structural Dynamics* **32** (10), 1603–1626.

[14] SENCICO (2003): *Standard E.030 Seismic Design*. National Building Regulations, Lima, Peru. (In Spanish).

[15] Iervolino I, Galasso C and Cosenza E (2010): REXEL: computer aided record selection for code-based seismic structural analysis. *Bulletin of Earthquake Engineering* **8**, 339–362.

[16] Bommer JJ and Acevedo AB (2004): The use of real earthquake accelerograms as input to dynamic analysis. *Journal of Earthquake Engineering* **8** (4): 1–50.

[17] Mehanny SSF and El Howary HA (2010): Assessment of RC moment frame buildings in moderate seismic zones: Evaluation of Egyptian seismic code implications and system configuration effects. *Engineering Structures* **32**, 2394–2406.

[18] Alcocer SM, Arias J and Vazquez A (2004): Response assessment of Mexican confined masonry structures through shaking table tests. Proceedings of the *13th World Conference on Earthquake Engineering*, Vancouver, B.C., Canada. Paper No. 2130.

[19] Matsuzaki S, Pulido N, Yamanaka K, Chimoto K, Maruyama Y and Yamazaki F (2013): Vulnerability estimation of buildings using damage survey data following the 2007 Pisco, Peru, Earthquake. *Journal of Social Safety* **21** (In Japanese).

[20] SEAOC (1999): *Recommended Lateral Forces Requirements and Commentary (the Blue Book)*. Structural Engineers Association of California, California.

[21] Barbat AH, Carreño ML, Pujades LG, Lantada N, Cardona OD and Marulanda MC (2010): Seismic vulnerability and risk evaluation methods for urban areas. A review with application to a pilot area. *Structure and Infrastructure Engineering: Maintenance, Management, Life-Cycle Design and Performance* **6** (1–2), 17–38.

[22] ATC-21 (2001): *Rapid Visual Screening of Seismically Hazardous Buildings*. Applied Technology Council, Redwood City, CA.